# Connexin 50-R205G Mutation Perturbs Lens Epithelial Cell Proliferation and Differentiation

Nikki Tjahjono, Chun-hong Xia, Rachel Li, Sarah Chu, Jessica Wang, and Xiaohua Gong

School of Optometry, University of California, Berkeley, Berkeley, California, United States

Correspondence: Xiaohua Gong, 693 Minor Hall, University of California, Berkeley, Berkeley, CA 94720-2020, USA;
xgong@berkeley.edu.

NT and CX are co-first authors.

**Received:** July 24, 2019
**Accepted:** January 2, 2020
**Published:** March 17, 2020

Citation: Tjahjono N, Xia C-hong, Li R, Chu S, Wang J, Gong X. Connexin 50-R205G mutation perturbs lens epithelial cell proliferation and differentiation. *Invest Ophthalmol Vis Sci*. 2020;61(3):25.
https://doi.org/10.1167/iovs.61.3.25

**Purpose.** To investigate the underlying mechanisms for how the mouse Cx50-R205G point mutation, a homologue of the human Cx50-R198W mutation that is linked to cataract-microcornea syndrome, affects proper lens growth and fiber cell differentiation to lead to severe lens phenotypes.

**Methods.** EdU labeling, immunostaining, confocal imaging analysis, and primary lens epithelial cell culture were performed to characterize the lens epithelial cell (LEC) proliferation and fiber cell differentiation in wild-type and Cx50-R205G mutant lenses in vivo and in vitro.

**Results.** The Cx50-R205G mutation severely disrupts the lens size and transparency. Heterozygous and homozygous Cx50-R205G mutant and Cx50 knockout lenses all show decreased central epithelium proliferation while only the homozygous Cx50-R205G mutant lenses display obviously decreased proliferating LECs in the germinative zone of neonatal lenses. Cultured Cx50-R205G lens epithelial cells reveal predominantly reduced Cx50 gap junction staining but no change of the endoplasmic reticulum stress marker BiP. The heterozygous Cx50-R205G lens fibers show moderately disrupted Cx50 and Cx46 gap junctions while the homozygous Cx50-R205G lens fibers have drastically reduced Cx50 and Cx46 gap junctions with severely altered fiber cell shape in vivo.

**Conclusions.** The Cx50-R205G mutation inhibits both central and equatorial lens epithelial cell proliferation to cause small lenses. This mutation also disrupts the assembly and functions of both Cx50 and Cx46 gap junctions in lens fibers to alter fiber cell differentiation and shape to lead to severe lens phenotypes.

Keywords: gap junction, cataract, lens epithelial cells, lens growth

The lens is an avascular organ, composed of a monolayer of anterior epithelial cells that differentiate at the lens equator into elongated fiber cells, which make up the majority of the lens mass.[1,2] Intercellular gap junction channels provide pathways for transporting metabolites, ions, and fluid between lens epithelial and fiber cells, which are essential for maintaining lens homeostasis, as well as ensuring lens growth and transparency.[3–8] Gap junctions are highly specialized membrane structures formed by connexin proteins. Six connexin protein subunits oligomerize into hexameric hemichannels; these hemichannels then either become functional unopposed or dock with other hemichannels to form an intercellular channel.[9] Different connexin isoforms may form mixed hemichannels and gap junction channels (heteromeric/heterotypic), in addition to forming channels of one form (homomeric/homotypic). These channels cluster with each other to form gap junction plaques.

Rodent and human lenses mainly express three isoforms of connexin: Cx43 (Gja1), Cx46 (Gja3), and Cx50 (Gja8). Cx43 is primarily expressed in the lens epithelium, Cx46 mainly in the lens fiber cells, and Cx50 in both lens epithelial cells and fibers.[10–12] Both Cx50 knockout and Cx46 knock-in (in the Cx50 locus) mice have reduced lens size, but only knockout mice develop mild cataracts while knock-in mice display clear lenses.[7,13,14] These studies reveal the nonredundant essential functions of Cx46 in maintaining lens transparency and Cx50 in lens growth processes. Cx50 is one of the most abundant membrane proteins and the most highly expressed connexin isoform in the lens.[15] The Cx50 accounts for approximately 60% of lens epithelial gap junction coupling during the first week of lens growth, a period of time during which lens mass expands substantially due to increased lens epithelial cell proliferation, especially in the first two to three days of development.[7,8] Dysfunctional connexin 50 affects proper lens growth and fiber cell differentiation,[13,16] although the underlying mechanisms are not well understood. A recent study reports that Cx50-D47A, a point mutation occurring on extracellular loop 1 (E1) of the protein, decreases both Cx50 and Cx46 gap junction coupling in lens fibers and increases the gradients of intracellular hydrostatic pressure and calcium level, which leads to calcium precipitates and cataracts.[17]

Mouse Cx50-R205G mutation, on extracellular loop 2, displays semidominant ocular phenotypes that differed from Cx50 knockout and other Cx50 point mutations reported previously.[17–19] The Cx50-R205G heterozygous mice show reduced lens size and mild cataracts while homozygous mice develop much more severe phenotypes, including a much smaller lens with vacuole-like structures in lens cortical fibers and a dense nuclear cataract.[20] This

Copyright 2020 The Authors


This work is licensed under a Creative Commons Attribution-NonCommercial-NoDerivatives 4.0 International License.

mutation is homologous to the human Cx50-R198W, linked to cataract-microcornea syndrome.[21] Current study reveals that the Cx50-R205G mutation inhibits lens epithelial cell proliferation and disrupts fiber cell shape to lead to unique lens phenotypes. Decreased central epithelium proliferation occurs in both Cx50-R205G and Cx50-knockout mutant lenses; however, only the Cx50-R205G mutation shows decreased and aberrant distribution of proliferating lens epithelial cells (LECs) in the germinative zone near the lens equator. Furthermore, the Cx50-R205G mutant reduces gap junction formation and disrupts morphogenesis of equatorial differentiating cells and inner fiber cells. These results suggest that the Cx50-R205G mutant disrupts multiple functions of Cx50 and Cx46 to exclusively perturb epithelial cell proliferation and differentiation at the lens equator.

## Material and Methods

### Mice

All experimental procedures were approved by the Animal Care and Use Committee (ACUC) at University of California, Berkeley, and were conducted in accordance with the ARVO Statement for the Use of Animals in Ophthalmic and Vision Research. The Cx50-R205G mutant mouse line was generated from the original Nm2249 mutant mice in the CWXS/Ag1 strain background, bred with $Gja8^{TM1}Gja3^{TM1}$ double knockout mice[22] at C57BL/6J background and maintained at the mixed stain background of CWXS/Ag1 and C57BL/6J with normal CP49 gene allele.[20]

### EdU Labeling and Whole-Lens Fluorescent Analysis

EdU labeling of the lens in vivo was performed mainly based on a previous published procedure.[23] P2 or P3 neonatal pups were intraperitoneally injected with 50 µg/g 5-ethynyl-20-deoxyuridine (Click-iT EdU Alexa Fluor 488 Imaging Kit; Thermo Fisher Scientific, Waltham, MA, USA). Two hours following injection, pups were euthanized, and lenses were collected and fixed in 4% paraformaldehyde (PFA)/PBS for 45 minutes at 37°C. Subsequent staining reactions were performed according to the manufacturer's protocol. Z-stack images were then collected with a confocal microscope (Zeiss LSM 700; Zeiss, Jena, Germany). The ImageJ software (National Institutes of Health, Bethesda, MD, USA) was used to process the analysis of flatten Z-stack images, subtract background fluorescence, convert the image to 8-bit grayscale, and center the fluorescent region. For total fluorescence and line scan analysis, thresholding of the grayscale images was performed. Multiple line scans per image were taken along the diameter of each lens image, and pixel values were averaged at each position to generate line scan plots. Total fluorescent values were obtained by normalizing the area of the fluorescing region by individual lens diameters and taking the average of this ratio among the different samples.

### Immunohistochemistry and Whole-Lens Staining

Mouse lenses were dissected and fixed for 30 minutes in 4% PFA/PBS at 37°C. For histologic analysis, the lenses were cut into 100-µm sections with a Leica VT1000 S vibratome (Leica, Wetzlar, Germany). The sections were postfixed with 4% PFA/PBS for 2 minutes, then washed three times with PBS. For immunostaining, fixed lens vibratome sections or prepermeabilized whole lenses (20 minutes in 0.3% Trition X-100/PBS) were blocked with a solution of 3% BSA, 3% goat serum, and 0.3% Triton X-100 in PBS for 1 hour. Primary antibodies diluted in blocking solution were added for overnight at 4°C. Sections were then washed three times with PBS before incubating with rhodamine–wheat germ agglutinin or secondary antibodies at room temperature for 2 hours. After washing three times with PBS and an additional wash of deionized water, lens sections were mounted on glass slides with Vectashield antifade mounting medium (H-1200; Vector Laboratories, Burlingame, CA) with 4',6-diamidino-2-phenylindole (DAPI). For whole-lens staining, the secondary antibody incubation was prolonged to overnight at 4°C, lenses were washed, and nuclei were stained with DAPI and imaged with a Zeiss LSM 700 confocal microscope.

### Preparation of Lens Epithelial Cell Culture

The LEC culture was performed based on a previously published procedure.[24] Briefly, lenses were dissected in Dulbecco's modified Eagle's medium/Ham's F-12 (Advanced DMEM/F-12; Gibco Invitrogen, Waltham, MA) with 1% penicillin-streptomycin solution and incubated for 20 minutes in 0.05% Trypsin-EDTA. For each lens, the lens capsule was separated from its associated fiber cell mass and then incubated with the fiber cell mass in Dispase for 10 minutes. An equal volume of TrypLE (Gibco Invitrogen, Waltham, MA) was then added, and the mixture was incubated for 10 minutes for LEC dissociation. The cell suspension was retrieved and then pelleted at 1000 rpm for 5 minutes. The cells were then resuspended in SB medium containing Advanced DMEM/F-12 with 1% penicillin-streptomycin supplemented with Glutamax, 2% FBS, B-27 supplement, and 2 µm SB431542.[24] Cells were then plated in 35-mm glass-bottom plates or eight-well glass-bottom plates and incubated in the SB media.

### Immunocytochemistry Analysis of Cultured Mouse Lens Epithelial Cells

Cultured LECs were washed with Dulbecco's PBS to remove the medium and fixed in 4% PFA in PBS for 10 minutes. After washing the plates three times with PBS, the cells were incubated in the blocking solution for 1 hour. The primary antibodies used were a rabbit polyclonal antibody against the intracellular loop of Cx46 connexin prepared in the laboratory previously,[6] a rabbit polyclonal antibody against the C-terminal region of Cx50 connexin (generously provided by M. J. Wolosin, Mt Sinai School of Medicine, New York), a rabbit antibody against Cx43 connexin (Zymed Laboratories, South San Francisco, CA), and a rabbit antibody against GRP78 BiP (Abcam, Cambridge, MA). All primary antibodies were diluted 1:200 in blocking solution. The primary antibody solutions were applied overnight at 4°C. Cells were then washed four times and fluorescently labeled secondary antibodies were applied for 2 hours. Cells isolated from mice that were not GFP (green fluorescent protein) positive were labeled with goat anti-rabbit IgG-FITC (1:100 in blocking solution). The cells were then washed four times with PBS and a final wash of deionized water before Vectashield antifade mounting medium (H-1200; Vector Laboratories) with DAPI was applied. Images were collected with a Zeiss LSM 700 confocal microscope.

Investigative Ophthalmology & Visual Science

## Results

### Drastically Reduced Lens Size and Severe Nuclear Cataracts in Cx50-R205G Mutant Mice

At postnatal day 3 (P3), the homozygous Cx50 (R205G/R205G) lenses already developed dense nuclear cataracts and cortical vacuoles, and the lens size was noticeably much smaller than the wild-type and the Cx50(–/–) knockout lenses (Fig. 1A); the mild cataract in the Cx50 knockout was not obvious at P3. At the age of 3 weeks, the homozygous Cx50(R205G/R205G) lenses remained the smallest with severe nuclear cataracts and vacuole-like abnormal defects on the lens periphery, while the Cx50(–/–) knockout lenses had visible mild cataracts and were smaller than the Cx50(+/+) wild-type lenses (Fig. 1B). To compare the lens size, we measured the lens diameters, calculated the lens volume by assuming a spherical shape of each lens, and performed statistical analysis using the Student's *t*-test. At P3, compared with the wild-type control, the homozygous Cx50(R205G/R205G) lenses were approximately 40% smaller ($P < 0.001$), while the Cx50 knockout lenses were approximately 33% smaller ($P < 0.001$); the Cx50(R205G/R205G) mutant lenses were approximately 9% smaller than the knockout lenses ($P < 0.01$). By the age of P21, the homozygous Cx50(R205G/R205G) lenses showed approximately 64% size reduction ($P < 0.001$) compared with the wild-type lenses, and the knockout lenses were 39% smaller than the wild-type ($P < 0.001$); the homozygous Cx50(R205G/R205G) mutant lenses were approximately 41% smaller than the Cx50 knockout lenses ($P < 0.001$). Therefore, the Cx50-R205G mutation was uniquely detrimental to the neonatal lens development. Both female and male Cx50-R205G mutant mice had the same lens phenotypes.

To determine how the lens growth is affected by the Cx50-R205G mutation, we measured the mouse lens wet weight of different genotypes at ages from P3 to P42. The lens wet weight was recorded and plotted against the ages to generate the lens growth curve (Fig. 2A). By calculating the average lens weight (n = 3–7 mice for each genotype at each time point) and performing the Student's *t*-test, the homozygous Cx50(R205G/R205G) lenses showed the most severe reduction in the lens wet weight when compared with all other genotypes ($P < 0.001$, compared with wild-type, at all time points; $P < 0.001$, compared with heterozygous Cx50-R205G, at all time points except $P < 0.01$ at P3) (Fig. 2A), and the heterozygous Cx50(R205G/+) lenses had consistently lower lens weight, on average, than wild-type lenses at all postnatal timepoints ($P < 0.001$ at all time points except $P < 0.01$ at P7) (Fig. 2A). Moreover, the average lens weight of homozygous Cx50(R205G/R205G) mice was consistently lower than that of the Cx50(–/–) knockout lenses ($P < 0.05$ at P14 and $P < 0.001$ at all other time points), indicating the distinct mechanism of lens growth disruption caused by the Cx50-R205G mutation and the deletion of Cx50 in the knockout mutant lenses (Fig. 2A). Due to the lens rupture phenotype occurring in the homozygous Cx50(R205G/R205G) mice around weaning age, we were unable to obtain their lens wet weight beyond the age of 3 weeks. The disparity in lens wet weight between wild-type and Cx50 mutant lenses occurred early in development. At P3, while the average Cx50(–/–) lens mass was approximately 64% that of wild-type lenses ($P < 0.001$), the average Cx50(R205G/R205G) lens mass was only approximately 46% that of the wild-type ($P < 0.001$) (Fig. 2B). At P7, the Cx50(–/–) knockout lens mass was approximately 60% that of wild-type ($P < 0.001$), while the Cx50(R205G/R205G) lens was only approximately 35% of wild-type lens mass ($P < 0.001$) (Fig. 2B). At postnatal day 3, the heterozygous Cx50(R205G/+) lens mass was approximately 59% that of wild-type ($P < 0.001$) and, at postnatal day 7, approximately 82% of wild-type ($P < 0.01$). There was no significant difference in lens mass between heterozygous Cx50(R205G/+) and Cx50(–/–) knockout lenses at P3 ($P = 0.24$); at P7, compared with the wild-type control, the Cx50(–/–) lens mass was reduced by approximately 40% ($P < 0.001$) and the heterozygous Cx50(R205G/+) lens mass by approximately 18% ($P < 0.01$) (Fig. 2B), the Cx50(R205G/+) and Cx50(–/–) knockout lenses showed a significant difference between their lens mass ($P < 0.01$), and the knockout lenses had a 25% mass reduction. Thus, the Cx50-R205G point mutation uniquely inhibits the neonatal lens growth.

### Inhibition of Lens Epithelial Cell Proliferation in the Cx50-R205G Lenses

In order to understand the underlying mechanism for disrupted lens growth caused by the Cx50-R205G mutation, we performed EdU labeling on the Cx50 mutant mice. We especially chose ages of postnatal days 2 and 3 because the previous study reported that Cx50 knockout and Cx46/Cx50 knock-in lens sizes are directly related to the changes of LEC proliferation from P2 to P3 in vivo.[7] Wild-type lenses experienced a surge of epithelial cell proliferation at postnatal days 2 and 3. The small size of Cx50-deficient lenses is at least partially attributed to a significant reduction in mitotic activity in the central epithelium at P2 and P3.[7] EdU labeling was performed and results were collected from flattened Z-stack images of the lens anterior epithelium (Figs. 3A, 3B). Compared with the control Cx50(+/+) wild-type lenses, a pronounced decrease in mitotic activity (less EdU-labeled cells) occurred in the central epithelium of the Cx50(–/–) lenses (Figs. 3A, 3B). Unlike those of the wild-type or Cx50(–/–) knockout lenses, EdU-labeled cells were unevenly distributed around the equatorial regions of the Cx50(R205G/R205G) lens epithelium (Figs. 3A, 3B). Only the Cx50(R205G/R205G) epithelium showed an irregular EdU labeling pattern with lower proliferating cell patches from the equator to the center. At P2, the Cx50(R205G/R205G) lenses had an approximately 71% reduction (in comparison to wild-type, $P < 0.001$, Student's *t*-test) in total proliferation compared with a 38% reduction in total proliferation in P2 Cx50(–/–) knockout lenses (in comparison to wild-type, $P < 0.001$) (Fig. 3C), indicating a severe disruption in the global proliferation rate. At the age of P3, the Cx50(R205G/R205G) lenses increased cell proliferation, but still much lower than that of the wild-type lenses (approximately 51% reduction, $P < 0.001$) (Fig. 3C). The P3 Cx50(–/–) knockout lenses showed an approximately 63% reduction ($P < 0.001$) compared with the wild-type lenses, and the reduction between the knockout and Cx50(R205G/R205G) lenses was statistically significant ($P < 0.05$). The heterozygous Cx50(R205G/+) lenses showed a normal pattern of EdU-incorporated cells (Figs. 3A, 3B) but lower total proliferation than the wild-type control (approximately 22% and 26% reductions of wild-type P2 and P3 lenses, respectively; $P < 0.001$), indicating the presence of one mutant allele of Cx50-R205G

Investigative Ophthalmology & Visual Science

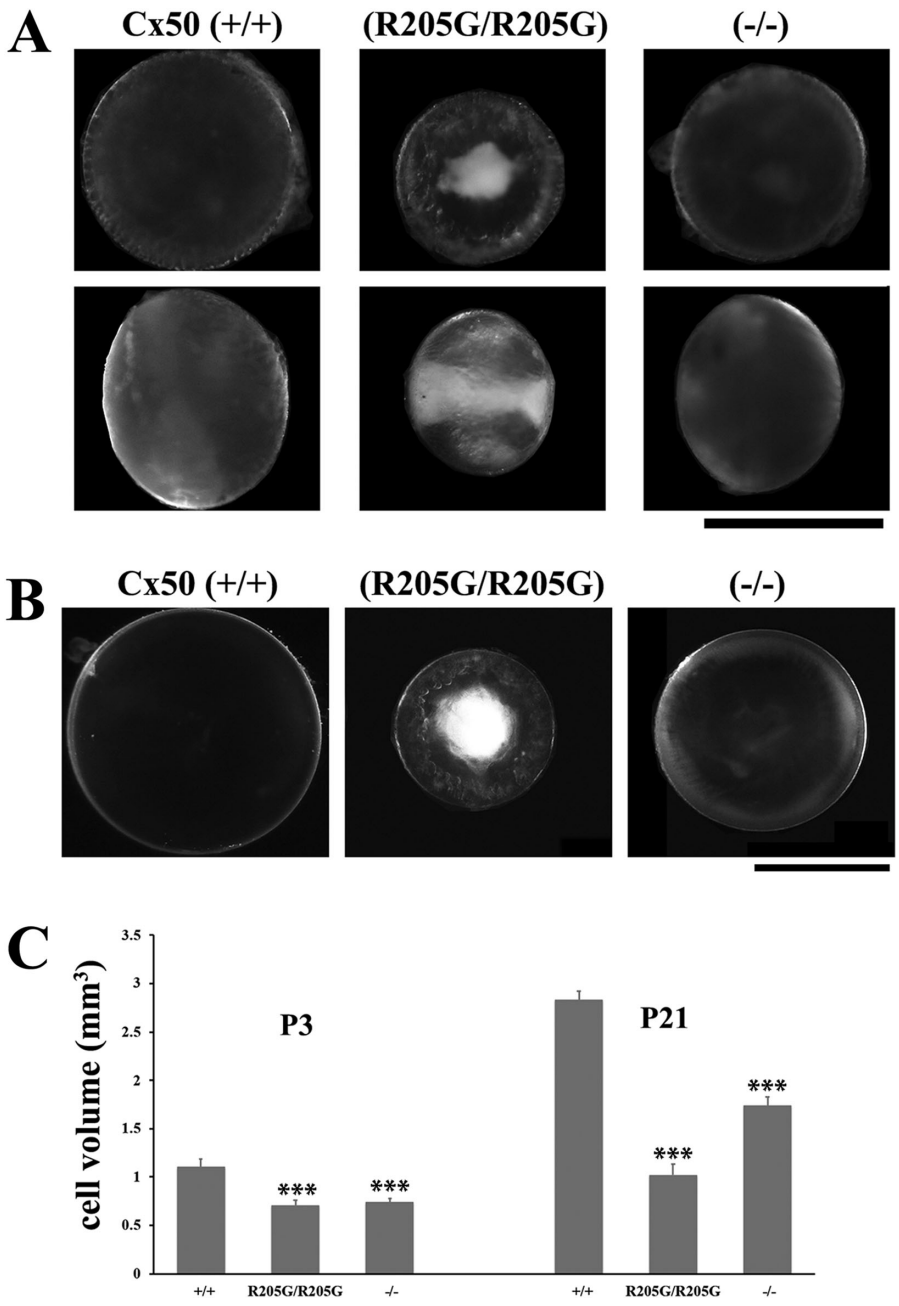


**Figure 1.** The homozygous Cx50(R205G/R205G) mutant lenses show more severe phenotype than the Cx50(–/–) knockout lenses. (**A**) Lens images of postnatal day 3 (P3) mice reveal early-onset growth defect and severe cataract in the homozygous Cx50(R205G/R205G) mutant lens, in comparison to the Cx50(+/+) wild-type and the Cx50(–/–) knockout lenses. The *upper panels* show lenses viewed from the anterior surface, while the *lower panels* display lenses viewed from the equator, and the anterior-posterior axis is from *left* to *right*. *Scale bar*: 1 mm. (**B**) Anterior view of fresh lenses of 3-week-old Cx50(+/+) wild-type, homozygous Cx50(R205G/R205G) and Cx50(–/–) knockout mice. *Scale bar*: 1 mm. (**C**) Lens volume comparison of P3 and P21 wild-type, homozygous Cx50(R205G/R205G), and Cx50(–/–) knockout mice. The P3 homozygous Cx50(R205G/R205G) lenses show approximately 40% reduction ($P < 0.001$) and the Cx50(–/–) knockout lenses have approximately 33% reduction ($P < 0.001$) when compared with the wild-type control. At P21, homozygous Cx50(R205G/R205G) lenses are approximately 64% smaller ($P < 0.001$) and the Cx50(–/–) knockout lenses are approximately 39% smaller ($P < 0.001$) than the wild-type lenses. Data are mean ± SD, $n = 6$–8 lenses of each genotype, with the Student's *t*-test for statistical analysis, ***$P < 0.001$, indicating statistically significant when compared with the wild-type.

inhibited the lens growth (Fig. 3C), but less severe than the homozygous mutants, displaying the semidominant nature of the Cx50-R205G mutation.

By quantitatively acquiring total fluorescence values through the line scans along the diameter of the flattened EdU images, we found that EdU-labeled epithelial cell proliferation was greatly reduced in the Cx50(R205G/R205G) lenses (Fig. 4); moreover, the pattern of EdU labeling was irregular in distribution across the mutant lens epithelium. At P2, the germinative zones near the equator of the Cx50(–/–) knockout (Fig. 4B) and wild-type (Fig. 4A) lenses had high and similar proliferation levels ($P > 0.5$, Student's *t*-test),

Investigative Ophthalmology & Visual Science

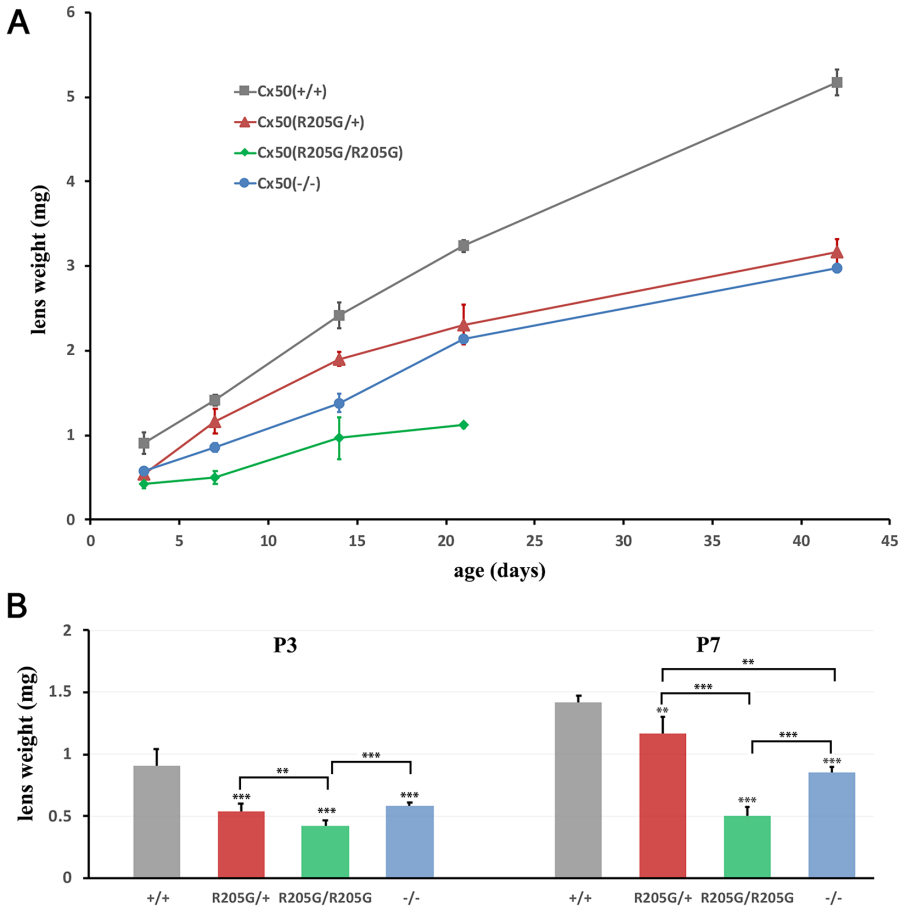


**Figure 2.** The lens growth curves of Cx50(+/+) wild-type, Cx50(–/–) knockout, heterozygous Cx50(R205G/+), and homozygous Cx50(R205G/R205G) lenses based on the lens wet weight at postnatal ages. (**A**) Individual wet lens weight was measured, and the average lens wet weight was obtained from mice of each genotype ($n$ = 3–7 mice). The average lens weight for each genotype was plotted at each age point from P3 to P42 days. The Cx50-R205G mutation displays a semidominant inheritance pattern, in which the heterozygous Cx50(R205G/+) lenses are smaller than the wild-type Cx50(+/+) lenses, while the homozygous Cx50(R205G/R205G) lenses are the smallest. (**B**) Statistical analysis and the wet weight bar graphs of different lenses at P3 and P7. Compared to the wild-type lenses, the P3 Cx50(–/–) lenses have approximately 36% reduction ($P < 0.001$), heterozygous Cx50(R205G/+) lenses show approximately 41% reduction ($P < 0.001$), and homozygous Cx50(R205G/R205G) lenses display approximately 54% reduction ($P < 0.001$); at P7, the Cx50(–/–) knockout lenses show approximately 40% reduced weight ($P < 0.001$), the heterozygous Cx50(R205G/+) lenses have approximately 18% reduction ($P < 0.01$), and homozygous Cx50(R205G/R205G) lenses have approximately 65% reduction ($P < 0.001$). The mean values per data point are presented as ± SD ($n$ = 3–10 mice). Student's $t$-test was used for statistical analysis, $^{**}P < 0.01$, $^{***}P < 0.001$, indicating statistically significant for the comparison.

evidenced by the two peaks in the line scan curves (Figs. 4A, 4B). However, compared with the wild-type control, the Cx50(R205G/R205G) lenses displayed an approximately 61% decrease on average in peak fluorescence, indicating fewer proliferating cells at germinative zones ($P < 0.01$) (Fig. 4A). Moreover, P2 Cx50(R205G/R205G) lenses had even lower proliferation at the central epithelium than the Cx50(–/–) knockout lenses ($P < 0.01$) (Fig. 4B). P3 Cx50(R205G/R205G) line scan data also showed the reduced proliferation near the equator ($P < 0.01$) but normal proliferation in the center (Fig. 4C). Therefore, the Cx50(–/–) null mutant lenses displayed an inhibition of central epithelial cell proliferation, while the Cx50(R205G/R205G) lenses showed severe inhibition of equatorial epithelial cell proliferation at germinative zones. These results indicate that the Cx50-R205G mutant seems to have a dominant effect on equatorial epithelial cells that may be related to the functions of Cx50 interacting proteins such as Cx46, Cx43, and/or ER (endoplasmic reticulum) stress associated with an accumulation of Cx50-R205G mutant proteins.

## Mutant Cx50-R205G Alters Gap Junctions Composed by Cx46, Cx50, and Cx43 in Lens Epithelial Cells In Vitro

To address the dominant effect of Cx50-R205G mutant proteins in equatorial epithelial cells, we used a mouse LEC culture system, which recapitulates the properties of equatorial epithelial cells.[24] To examine the effect of mutant Cx50-R205G on proper gap junction assembly, LECs were isolated, cultured, and stained with specific connexin antibodies. The LEC morphology appeared to be similar among all cells isolated from Cx50(+/+) wild-type, Cx50(–/–), and Cx50(R205G/R205G) mice (Fig. 5A). Expression of Cx46 is known to be turned on in the

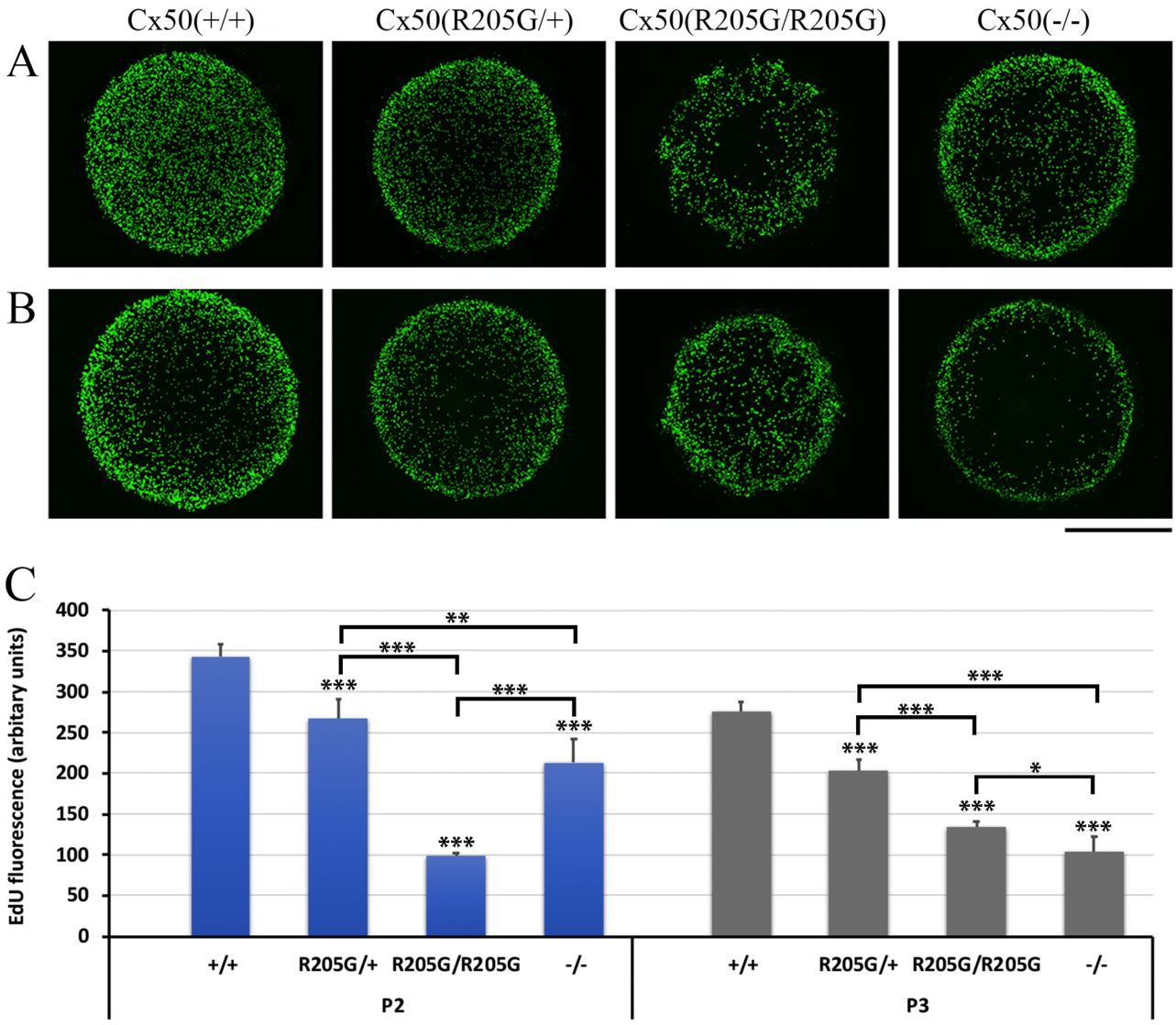


**Figure 3.** The Cx50-R205G mutation disrupts lens epithelial cell proliferation based on EdU labeling examination of P2 and P3 lenses in vivo. (**A**) Flattened Z-stack images of EdU-labeled lens epithelium of P2 mice. Compared with the wild-type Cx50(+/+), the heterozygous Cx50(R205G/+), the homozygous Cx50(R205G/R205G), and the Cx50(–/–) knockout lenses show reduced EdU labeling in central epithelium, while homozygous Cx50(R205G/R205G) lens also displays severely abnormal EdU labeling in peripheral epithelium (equator/germinative zone or GZ). (**B**) Flattened images of EdU-labeled lens epithelium of P3 mice. The homozygous Cx50(R205G/R205G) mutant has aberrant GZ proliferating cells with increased EdU labeling in the central epithelium (in comparison to P2 homozygous Cx50-R205G), the heterozygous Cx50(R205G/+) mutant lenses show increased EdU labeling in all epithelia, and the Cx50(–/–) knockout lens shows low EdU labeling in central epithelium. *Scale bar* (**A**, **B**), 500 µm. (**C**) Statistical comparison and bar graphs of EdU fluorescence in the Cx50-R205 mutant, Cx50-knockout, and wild-type lenses. Average EdU fluorescence, which correlates to proliferating epithelial cells, is obtained by determining the area of the fluorescent region of each flattened image and normalized by lens diameter. Compared with the wild-type control, among the homozygous Cx50(R205G/R205G), the heterozygous Cx50(R205G/+), and the Cx50(–/–) knockout, the homozygous Cx50(R205G/R205G) mutant mice have the most reduced total EdU fluorescence at P2 (approximately 71% reduction, $P < 0.001$), and the Cx50(–/–) knockout lenses display the most reduced total EdU fluorescence at P3 (approximately 63%, $P < 0.001$). Data presented as mean ± SD, $n = 3$–5 samples per data point, Student's *t*-test for statistical analysis. $^{*}P < 0.05$, $^{**}P < 0.01$, $^{***}P < 0.001$, indicating statistically significant when compared with the wild-type or compared as indicated.

equatorial epithelial cells based on the knock-in/lacZ reporter.[13] As we expected, immunostaining revealed that Cx46, Cx50, and Cx43 formed typical punctate gap junction plaques at cell-cell junctions in cultured wild-type LECs (Fig. 5B). The Cx50(–/–) knockout cells displayed punctate Cx46 plaques, similar to the wild-type control, but the Cx46 staining seemed to show weak and small/less plaques in the Cx50(R205G/R205G) epithelial cells (Fig. 5B); however, quantitation of Cx46 staining by ImageJ revealed no statistically significant difference between Cx50(R205G/R205G) and wild-type cells ($P > 0.05$, Student's *t*-test). In comparison to the typical dense/large Cx50 plaques between wild-type LECs (Fig. 5B), the Cx50(R205G/R205G) LECs showed many weak (nonpunctate plaques) Cx50 junctions at cell-cell contacts but no punctate dense plaques (Fig. 5B, upper middle image). ImageJ quantitation revealed significantly reduced Cx50 gap junction staining ($P < 0.01$) in the Cx50(R205G/R205G) cells when compared with

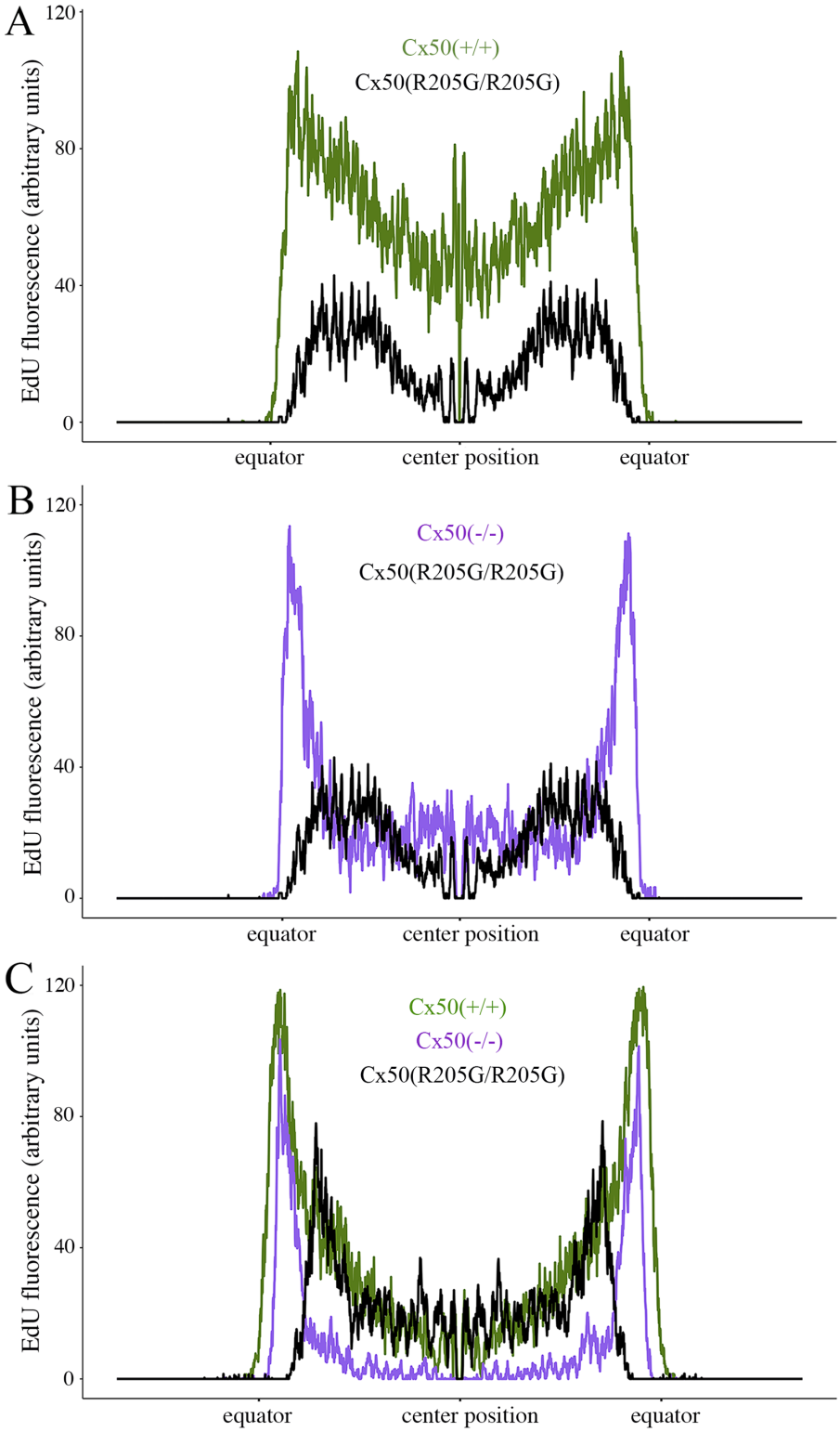


**Figure 4.** Quantification of EdU labeling from the peripheral (equator/germinative zone) to the central epithelium of P2 and P3 lenses. (**A**) Line scans along the flattened EdU fluorescent images of P2 lenses, crossing through the diameter of the lens (a position of approximately 1500 µm is the center of the lens, and the position at which the fluorescence jumps from zero is the lens equator). The P2 Cx50(R205G/R205G) lens has lower epithelial cell proliferation by EdU labeling at all locations along the lens diameter compared with the P2 wild-type Cx50(+/+) ($P < 0.01$). (**B**) A comparison of line scans of EdU-labeled P2 Cx50(–/–) knockout and P2 Cx50(R205G/R205G) lenses. The P2 Cx50(R205G/R205G) lens has significantly lower proliferation in both central and peripheral (germinative zone) epithelium compared with the P2 Cx50(–/–) ($P < 0.01$). (**C**) Line scan comparison of EdU-labeled P3 wild-type Cx50(+/+), Cx50(–/–), and Cx50(R205G/R205G) lenses. The P3 Cx50(R205G/R205G) lens has a surge in proliferation but still shows decreased proliferation in peripheral epithelium when compared with that of both wild-type and Cx50(–/–) ($P < 0.01$). For all line scan charts, about 154 to 166 line scans per sample were averaged for each age and genotype ($n = 3$–5); SEM ribbon not shown due to large sample size and small SE. Student's *t*-tests for the central epithelium performed at positions 1250 to 1750 µm.

Investigative Ophthalmology & Visual Science

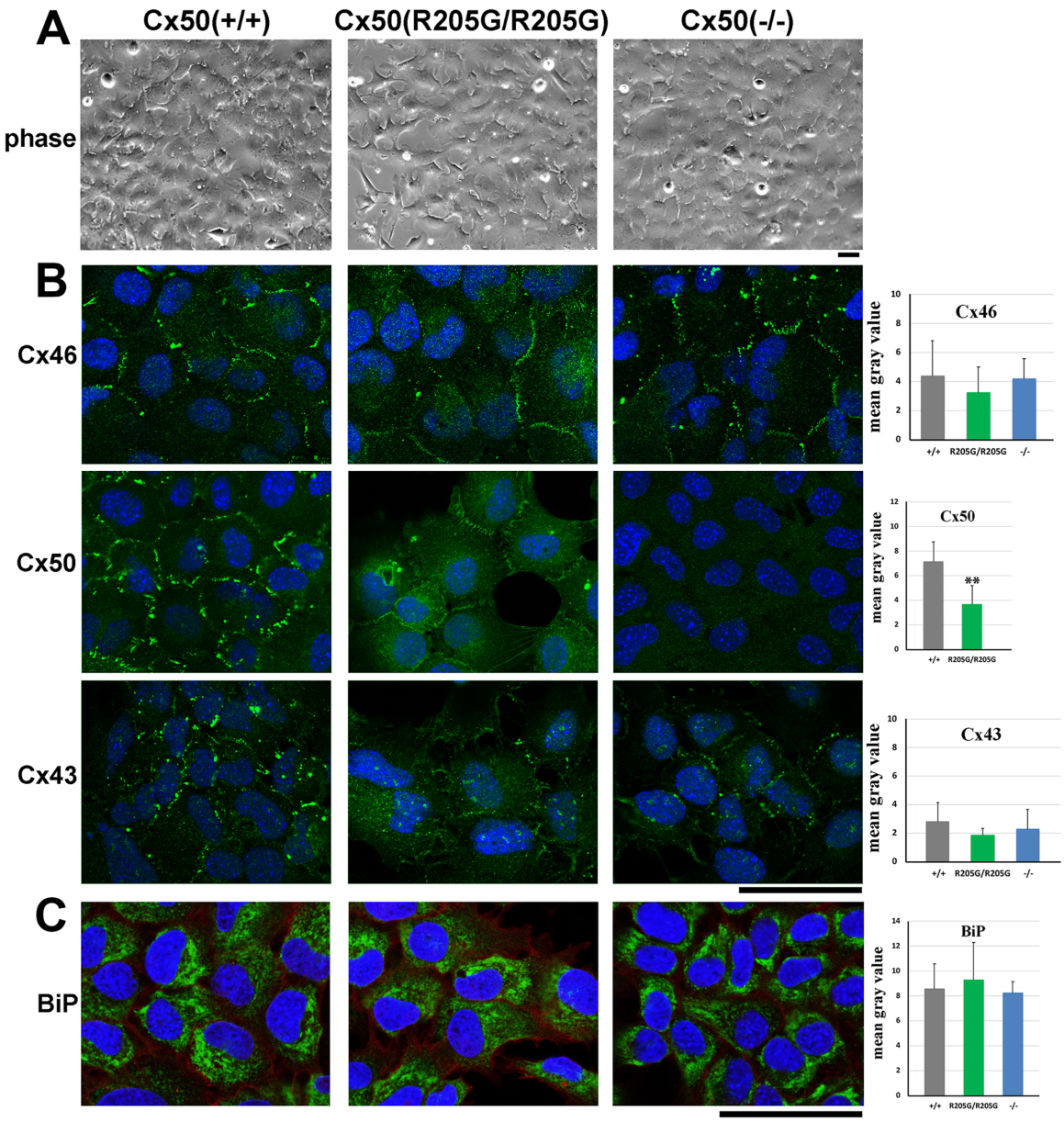


**Figure 5.** The Cx50 gap junctions are significantly reduced in cultured Cx50(R205G/R205G) primary lens epithelial cells in vitro. (**A**) No apparent morphologic difference is observed in cultured primary lens epithelial cells isolated from lenses of wild-type Cx50(+/+), Cx50(R205G/R205G), and Cx50(–/–) knockout mice. *Scale bar*: 50 µm. (**B**) Immunostaining of cultured primary lens epithelial cells with anti-Cx46, anti-Cx50, and anti-Cx43 antibodies (*green signals*, costained with DAPI in *blue*). Compared with the typical Cx46 (*green*) gap junctions at the cell-cell boundary of wild-type cells, reduced Cx46 gap junctions occurred in some Cx50(R205G/R205G) lens epithelial cells, while normal Cx46 junctions appeared in the Cx50(–/–) lens epithelial cells; however, quantitation of Cx46 staining by ImageJ reveals no statistically significant difference between Cx50(R205G/R205G) and wild-type cells ($P > 0.05$, Student's *t*-test). Compared with robust Cx50 gap junctions at the cell-cell boundary of wild-type lens epithelial cells, faint and thin Cx50 gap junctions are detected in the Cx50(R205G/R205G) lens epithelial cells and no Cx50 gap junction in Cx50(–/–) lens epithelial cells. Statistical analysis reveals significantly reduced Cx50 gap junction staining in Cx50(R205G/R205G) cells (**$P < 0.01$, mean ± SD, Student's *t*-test). Typical punctate Cx43 gap junctions are detected in wild-type epithelial cells, and Cx43 staining signal appears to be slightly reduced in the Cx50(R205G/R205G) and Cx50(–/–) lens epithelial cells; however, the Cx43 gap junction staining difference between wild-type and Cx50(R205G/R205G) cells is not statistically significant ($P = 0.16$). The bar graphs show quantitation of the membrane-stained connexin signal intensity by ImageJ. Three 63× images of staining were converted to grayscale and staining intensity was measured on five to six cells of each image; average mean gray intensity of each cell subtracted from background was plotted. Cell culture and staining were repeated at least three times, and similar results were observed. (**C**) Immunostaining of cultured primary lens epithelium cells with an anti-BiP antibody (BiP signal, *green*; DAPI, *blue*). BiP expression was detected in cytosols of all cells, enriched in endoplasmic reticulum. The bar graphs display quantitation of BiP signal intensity by ImageJ. Compared with the wild-type cells, the Cx50(R205G/R205G) and Cx50 knockout cells show comparable BiP expression; the differences are not statistically significant ($P > 0.05$, mean ± SD, Student's *t*-test). *Scale bar*: (**B**, **C**) 50 µm.

the wild-type cells. No Cx50 staining was detected in Cx50(–/–) knockout cells with the same anti-Cx50 antibody (Fig. 5B). Compared with wild-type LECs that displayed typical large punctate Cx43 signals between cells (Fig. 5B), Cx50(R205G/R205G) LECs appeared to have reduced and weak staining signals of the Cx43 staining (Fig. 5B); however, the quantitation of Cx43 gap junction staining intensity revealed that the reduction was not statistically significant ($P = 0.16$) (Fig. 5B, bar graphs). These results suggest that mutant Cx50-R205G inhibits gap junctions of endogenous Cx50 and may also affect Cx46 and Cx43 connexin in cultured LECs.

Previous studies have reported that Cx50-S50P, Cx50-G22R, and Cx50-D47A mutations can increase ER stress.[25,26] We examined the expression of BiP, an ER protein whose increased expression can reflect the activation of unfolded protein response, to test whether ER stress is a possible underlying mechanism for the severe cataracts caused by the Cx50-R205G mutation. Immunostaining of BiP was performed in primary cultured LECs (Fig. 4C), and its expression was quantified using ImageJ. The BiP staining signals were similar among the wild-type, Cx50(R205G/R205G), and Cx50(–/–) cells, present in cell cytosols with enriched expression in endoplasmic reticulum. ImageJ quantitation revealed that the BiP expression levels were comparable among the Cx50(R205G/R205G), Cx50(–/–), and wild-type cells ($P > 0.05$).

### Mutant Cx50-R205G Disrupts Fiber Cell Morphology and Gap Junction Formation In Vivo

To further understand the severe cataract phenotype in the Cx50(R205G/R205G) lens fibers, vibratome sections of wild-type, heterozygous, and homozygous Cx50-R205G mutant lenses from mice carrying a transgenic GFP allele (displaying GFP-positive epithelial and fiber cells)[27] were prepared for characterizing lens fiber cell morphology (Fig. 6A). These GFP-positive lens sections were also stained with rhodamine-labeled wheat germ agglutinin for plasma membrane. In the lens cross section from 3-week-old GFP-positive Cx50(+/+) wild-type mice, organized rows of hexagonal cortical fiber cells were observed; heterozygous Cx50(R205G/+) lens section had similar organized hexagonal cells; however, homozygous Cx50(R205G/R205G) section displayed irregularly/roundly shaped fibers with misaligned fiber-to-fiber organization (Fig. 6A). Moreover, unlike wild-type control showing aligned meridional rows of lens equatorial cells and a straight line of lens fulcrum (the apical tip of equatorial elongating epithelial cells),[28,29] the Cx50(R205G/R205G) homozygous mutant lens showed misaligned meridional rows and disrupted fulcrum line (Fig. 6B).

Lens gap junction distribution has been characterized in lens cross sections with anti-Cx46 and anti-Cx50 antibodies. Typical punctate gap junctions were detected on both the short and long sides, including the ball-and-socket structures of hexagonal shape fiber cells, in the Cx50(+/+) wild-type lens section (Figs. 6C, 6D). Heterozygous Cx50(R205G/+) lens section staining revealed reduced Cx46 and Cx50 gap junctions on both the short and long sides of the fiber cells and absence of typical ball-and-socket structures, but aberrant membrane structures with rounded heads and pinched necks appeared frequently in the superficial cortex (approximately 70 to 200 µm from the lens periphery) where the ball-and-socket structures would usually be enriched. Moreover, homozygous Cx50(R205G/R205G) lens section displayed sparse dots of Cx46 and Cx50 staining in roundly deformed fiber cells (Figs. 6C, 6D). The staining intensity of Cx46 and Cx50 was quantified using ImageJ (Fig. 6E), and the bar graphs of staining intensity revealed that the Cx50(R205G/R205G) lens had reduced Cx46 ($P < 0.001$) and Cx50 ($P < 0.001$) expression compared with the wild-type lens; the heterozygous Cx50(R205G/+) lens had reduced Cx50 ($P < 0.01$) expression, but its Cx46 expression ($P > 0.05$) was comparable to the wild-type. Thus, mutant Cx50-R205G impairs both Cx50 and Cx46 cell-cell gap junctions and disrupts the ball-and-socket structures in lens fiber cells. Disrupted lens fulcrum and misaligned meridional rows of Cx50(R205G/R205G) lenses reveal an effect of R205G mutant proteins on the differentiation and organization of equatorial cells.

## Discussion

This study reports mouse Cx50-R205G, a point mutation on extracellular loop 2 of the Cx50 protein,[20] reduces gap junction plaque formation in cultured Cx50-R205G LECs in vitro and in fiber cells in vivo, as well as evidence of disrupted lens fulcrum and misaligned meridional rows at lens equator and deformed fiber cells. Microphthalmia with small lens size of the Cx50-R205G mutant mice is associated with decreased central epithelium proliferation early in development, as well as obviously perturbed proliferating LECs in the germinative zone, a phenomenon not observed in the Cx50 knockout deficient lenses. Mutant Cx50-R205G not only impairs the assembly of normal Cx50 gap junctions but also disrupts the assembly of Cx46 gap junctions in lens fibers. Thus, this work reveals some novel mechanistic information for understanding the human homologous mutation Cx50-R198W that is linked to cataract-microcornea syndrome.[21]

Cx50 has been implicated in multiple studies to be essential for both fiber cell differentiation and epithelial cell proliferation.[7,12] Similar to Cx50-knockout deficient lenses, homozygous Cx50-R205G mutant lenses seem to have decreased central epithelium proliferation at postnatal days 2 and 3 of development. However, Cx50-R205G homozygous lenses also appear to have reduced equatorial epithelial cell proliferation with disrupted spatial distribution, despite having some Cx50 membrane localization. Our previous study has shown that mutant Cx50-R205G proteins alone are unable to form functional channels, and heterotypic Cx50-R205G and Cx46 channels are not electrically coupled in vitro. However, heteromeric Cx50-R205G and Cx46 channels do have normal conductance with altered gating properties, and the steady-state reduction in conductance for heteromeric Cx46 and Cx50-R205G channels is greater than the reduction for homomeric wild-type Cx46 channels.[20] The recently published mouse LEC culture condition[24] actually allows us to examine the distribution of endogenous Cx50 and Cx46 for the first time. Based on the evidence that Cx46 is expressed in the equatorial epithelial cells[13] and the potential alterations of Cx46 gap junctions in cultured Cx50-R205G epithelial cells (Fig. 5), it is possible that Cx50-R205G uniquely disrupts the Cx46/Cx50 gap junction dependent property in lens equatorial cells to lead to drastic inhibition of equatorial epithelial cell proliferation, disruption of lens fulcrum, and misaligned meridional rows.

Investigative Ophthalmology & Visual Science

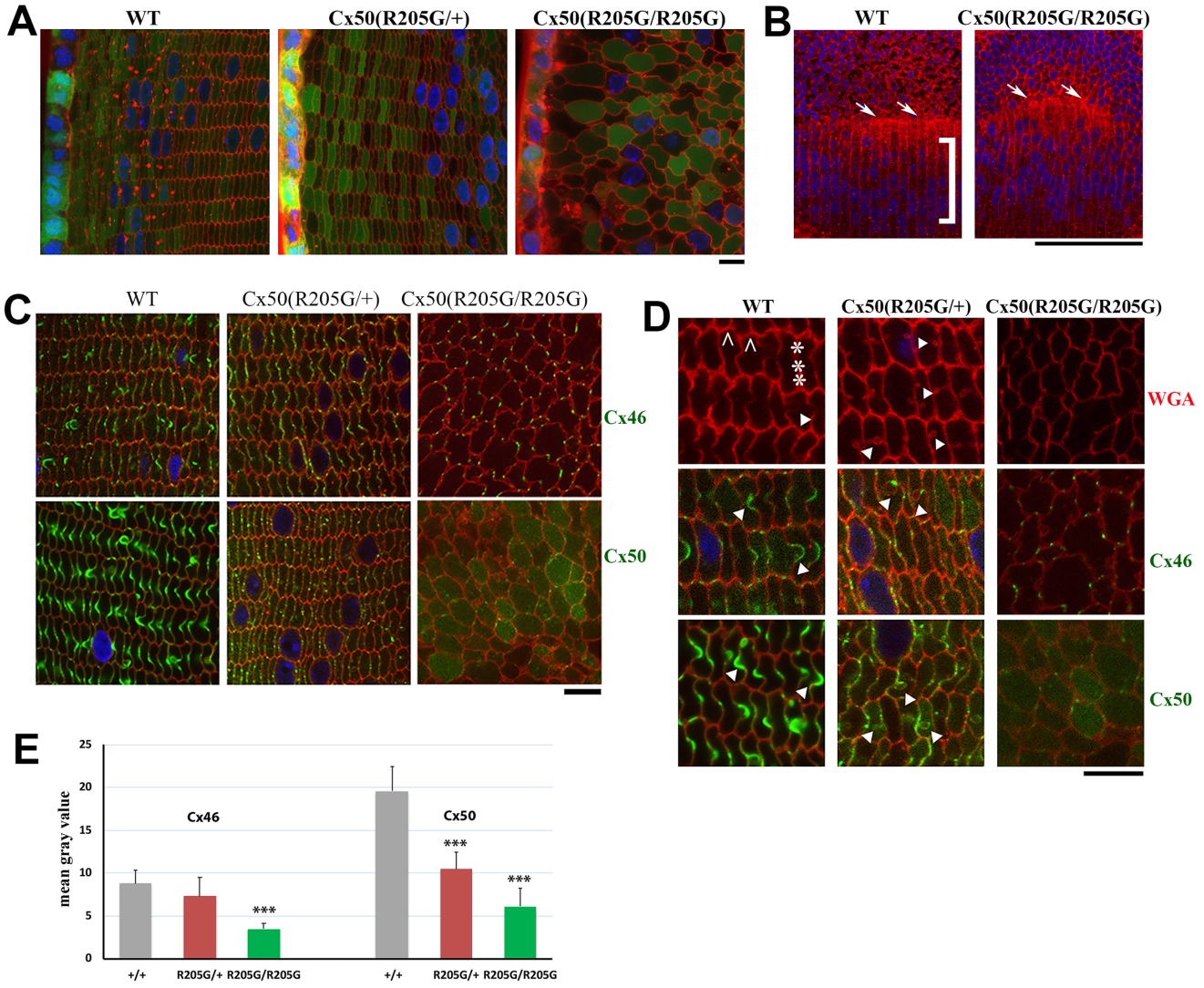


**Figure 6.** The Cx50-R205G mutation disrupts meridional rows and fulcrum at lens equator and alters lens fiber cell shape and gap junctions. (**A**) Lens fiber cell morphology revealed by wheat germ agglutinin (WGA; *red*) and DAPI (*blue*) stained cross sections of GFP-positive (*green*) Cx50(+/+) wild-type, Cx50(R205G/+), and Cx50(R205G/R205G) lenses from 3-week-old mice. Images collected from the lens periphery to interior 100-µm fibers are displayed. The heterozygous Cx50-R205G lens fiber cells show hexagonal cell shape with normal fiber-to-fiber overlay organization while homozygous Cx50-R205G lens fiber cells display rounded cell shape and irregular organization. *Scale bar*: 10 µm. (**B**) Equatorial images of P13 wild-type and Cx50(R205G/R205G) lenses stained with WGA (*red*) and DAPI (*blue*). In the wild-type lens, meridional rows (indicated by ]) are aligned and straight, but the meridional rows of Cx50(R205G/R205G) lenses are misaligned. The Cx50(R205G/R205G) lens fulcrum (indicated by *white arrows*) is disrupted, unlike the straight line of the wild-type lens fulcrum (*white arrows*). *Scale bar*: 100 µm. (**C**) Cx46 and Cx50 gap junction expression in lens sections costained with either anti-Cx46 or anti-Cx50 antibodies (*green*), WGA (*red*), and DAPI (*blue*). In the wild-type lens, Cx46 and Cx50 gap junction plaques are enriched in the ball-and-sockets and also expressed on the long and narrow sides of fibers. Heterozygous Cx50-R205G fiber cells display reduced and short or small gap junction plaques along the broad and short sides, while the homozygous Cx50(R205G/R205G) fibers only have sparse, very short, or dot-like Cx46 and Cx50 plaques. All lens sections were from 3-week-old mice. *Scale bar*: 10 µm. (**D**) Enlarged images of lens fibers costained with anti-Cx46 or anti-Cx50 (*green*), WGA (*red*), and DAPI (*blue*). Typical Cx46 and Cx50 gap junctions are detected in wild-type ball-and-sockets (indicated by *white arrowheads*) while short or dot-like Cx46 and Cx50 signals are observed in Cx50(R205G/+) fiber cell boundaries with aberrant membrane structures (indicated by *arrowheads*). The *caret* indicates the short side of the hexagonal shaped fibers in the wild-type, while the *asterisk* marks the long side. All lens sections were from 3-week-old mice. *Scale bar*: 10 µm. (**E**) Bar graphs of Cx46 and Cx50 staining intensity quantitation. Compared with the wild-type lens section staining, the Cx50(R205G/R205G) section shows significantly reduced Cx46 ($P < 0.001$) and Cx50 ($P < 0.001$) staining intensity; the heterozygous Cx50(R205G/+) displays significantly reduced Cx50 staining intensity ($P < 0.001$) compared with the wild-type, but the difference of Cx46 staining intensity between the heterozygous and wild-type is not statistically significant ($P = 0.27$). Data are shown as mean ± SD, Student's *t*-test, ***$P < 0.001$, indicating statistically significant when compared with the wild-type.

We are unclear about whether a non-junction-dependent property of Cx50 extracellular loop 2 may imply the underlying mechanism severely disrupts epithelial cell proliferation by the Cx50-R205G mutation. Cx50 is implicated in playing crucial roles of cell cycle regulation independent of cell-cell communication by regulating the degradation of E3 ligase Skp2 in Cx50 knockout lenses.[30] It is possible that Cx50 non-junction-dependent function influences the inhibition

Investigative Ophthalmology & Visual Science

of central epithelial cells. However, it seems unlikely to be the case for the homozygous Cx50(R205G/R205G) mutant lens that is obviously smaller than the Cx50(–/–) knockout lens by drastically inhibiting proliferation of equatorial epithelial cells. A recent study also indicates that the second extracellular loop domain (E2) of Cx50 is primarily responsible for adhesive function in lens cell differentiation. The E2 loop is believed to mediate cell-cell adhesion with AQP0 and affect normal epithelial cell differentiation, and disrupted cell adhesion by the E2 domains impairs primary lens cell differentiation in vitro.[31] It is possible that the E2 domain of Cx50-R205G may alter the adhesive function of Cx50 as one of its multiple functions to further impair epithelial-fiber differentiation and lens fiber integrity in addition to altered gap junction communication. Furthermore, we observed a disrupted lens fulcrum, where the elongating tips of epithelial cells anchor before further fiber cell differentiation,[28] which may be related to cell adhesion and/or differentiation defects.

Many Cx50 mutations with a variety of lens phenotypes have been reported. The Cx50-D47A, Cx50-G22R, and Cx50-S50P mutations have improper and reduced gap junction communication in the lens and have been implicated in inducing stress pathways or promoting calcium elevation and deposits.[17,25,26] Increased ER stress is also involved in the cell death in skin disease-associated Cx31 mutations.[32,33] However, our data indicate that the BiP expression is not significantly increased, and there is no obvious accumulation of Cx50-R205 mutant proteins in cultured Cx50(R205G/R205G) LECs (Fig. 5C), suggesting ER stress may not be a key factor for the severe cataract formation. It seems to be true that altered gap junction may contribute to the severely disrupted fiber cell morphology in the Cx50-R205G mutants like that of the Cx50-D47A mutants. In the Cx50-R205G heterozygous lenses, we also observed disrupted ball-and-socket-like membrane structures with reduced gap junctions. These structures appear to be very similar to the structures seen previously in Cx50(Cx46/Cx46) knock-in and Cx50(–/–) lenses,[34] indicating that one allele of Cx50-R205G is sufficient to cause the same phenotype of reduced fiber cell communication and perturbed fiber cell maturation observed in Cx50(–/–) deficient lenses. This characteristic change, as well as the lack of ball-and-socket-like structures and disrupted lens fulcrum observed in Cx50(R205G/R205G) lenses, implicate that mutant Cx50-R205G perturbs fiber cell differentiation in addition to epithelial cell proliferation. Thus, the Cx50-R205G probably impairs multiple functions of Cx50 to lead to severe nuclear cataracts and decreased lens size. Cx50 has been shown to respond to PI3K (phosphoinositide 3-kinase) and MAPK (mitogen-activated protein kinase) pathway activation and regulates cell cycle modulators such as p27/p57, thus having important implications in lens cell fate determination.[30,35,36] Further studies will be needed to determine additional mechanisms of Cx50 mutants in lens growth regulation.

## Acknowledgments

Supported by National Institutes of Health R01 EY013849 (XG).

Disclosure: **N. Tjahjono**, None; **C.-hong Xia**, None; **R. Li**, None; **S. Chu**, None; **J. Wang**, None; **X. Gong**, None

## References

1. Piatigorsky J. Lens differentiation in vertebrates: a review of cellular and molecular features. *Differentiation*. 1981;19:134–153.
2. Bassnett S, Sikic H. The lens growth process. *Prog Retin Eye Res*. 2017;60:181–200.
3. Mathias RT, Rae JL. The lens: local transport and global transparency. *Exp Eye Res*. 2004;78:689–698.
4. Mathias RT, White TW, Gong X. Lens gap junctions in growth, differentiation, and homeostasis. *Physiol Rev*. 2010;90:179–206.
5. Gong X, Cheng C, Xia CH. Connexins in lens development and cataractogenesis. *J Membr Biol*. 2007;218:9–12.
6. Gong X, Li E, Klier G, et al. Disruption of alpha3 connexin gene leads to proteolysis and cataractogenesis in mice. *Cell*. 1997;91:833–843.
7. Sellitto C, Li L, White TW. Connexin50 is essential for normal postnatal lens cell proliferation. *Invest Ophthalmol Vis Sci*. 2004;45:3196–3202.
8. White TW, Gao Y, Li L, Sellitto C, Srinivas M. Optimal lens epithelial cell proliferation is dependent on the connexin isoform providing gap junctional coupling. *Invest Ophthalmol Vis Sci*. 2007;48:5630–5637.
9. Evans WH, De Vuyst E, Leybaert L. The gap junction cellular internet: connexin hemichannels enter the signalling limelight. *Biochem J*. 2006;397:1–14.
10. Musil LS, Goodenough DA. Biochemical analysis of connexin43 intracellular transport, phosphorylation, and assembly into gap junctional plaques. *J Cell Biol*. 1991;115:1357–1374.
11. Paul DL, Ebihara L, Takemoto LJ, Swenson KI, Goodenough DA. Connexin46, a novel lens gap junction protein, induces voltage-gated currents in nonjunctional plasma membrane of *Xenopus* oocytes. *J Cell Biol*. 1991;115:1077–1089.
12. White TW, Bruzzone R, Goodenough DA, Paul DL. Mouse Cx50, a functional member of the connexin family of gap junction proteins, is the lens fiber protein MP70. *Mol Biol Cell*. 1992;3:711–720.
13. Rong P, Wang X, Niesman I, et al. Disruption of Gja8 (alpha8 connexin) in mice leads to microphthalmia associated with retardation of lens growth and lens fiber maturation. *Development*. 2002;129:167–174.
14. White TW. Unique and redundant connexin contributions to lens development. *Science*. 2002;295:319–320.
15. Bassnett S, Wilmarth PA, David LL. The membrane proteome of the mouse lens fiber cell. *Mol Vis*. 2009;15:2448–2463.
16. White TW, Goodenough DA, Paul DL. Targeted ablation of connexin50 in mice results in microphthalmia and zonular pulverulent cataracts. *J Cell Biol*. 1998;143:815–825.
17. Berthoud VM, Gao J, Minogue PJ, Jara O, Mathias RT, Beyer EC. The connexin50D47A mutant causes cataracts by calcium precipitation. *Invest Ophthalmol Vis Sci*. 2019;60:2336–2346.
18. Chang B, Wang X, Hawes NL, et al. A Gja8 (Cx50) point mutation causes an alteration of alpha 3 connexin (Cx46) in semi-dominant cataracts of Lop10 mice. *Hum Mol Genet*. 2002;11:507–513.
19. Xia CH, Liu H, Cheung D, et al. Diverse gap junctions modulate distinct mechanisms for fiber cell formation during lens development and cataractogenesis. *Development*. 2006;133:2033–2040.
20. Xia CH, Chang B, Derosa AM, Cheng C, White TW, Gong X. Cataracts and microphthalmia caused by a Gja8 mutation in extracellular loop 2. *PLoS One*. 2012;7:e52894.
21. Hu S, Wang B, Zhou Z, et al. A novel mutation in GJA8 causing congenital cataract-microcornea syndrome in a Chinese pedigree. *Mol Vis*. 2010;16:1585–1592.

22. Xia CH, Cheng C, Huang Q, et al. Absence of alpha3 (Cx46) and alpha8 (Cx50) connexins leads to cataracts by affecting lens inner fiber cells. *Exp Eye Res*. 2006;83:688–696.
23. Sellitto C, Li L, Vaghefi E, Donaldson PJ, Lin RZ, White TW. The phosphoinosotide 3-kinase catalytic subunit p110alpha is required for normal lens growth. *Invest Ophthalmol Vis Sci*. 2016;57:3145–3151.
24. Wang D, Wang E, Liu K, Xia CH, Li S, Gong X. Roles of TGFbeta and FGF signals during growth and differentiation of mouse lens epithelial cell in vitro. *Sci Rep*. 2017;7:7274.
25. Alapure BV, Stull JK, Firtina Z, Duncan MK. The unfolded protein response is activated in connexin 50 mutant mouse lenses. *Exp Eye Res*. 2012;102:28–37.
26. Berthoud VM, Minogue PJ, Lambert PA, Snabb JI, Beyer EC. The cataract-linked mutant connexin50D47A causes endoplasmic reticulum stress in mouse lenses. *J Biol Chem*. 2016;291:17569–17578.
27. Okabe M, Ikawa M, Kominami K, Nakanishi T, Nishimune Y. 'Green mice' as a source of ubiquitous green cells. *FEBS Lett*. 1997;407:313–319.
28. Sugiyama Y, Akimoto K, Robinson ML, Ohno S, Quinlan RA. A cell polarity protein aPKClambda is required for eye lens formation and growth. *Dev Biol*. 2009;336:246–256.
29. Cheng C, Ansari MM, Cooper JA, Gong X. EphA2 and Src regulate equatorial cell morphogenesis during lens development. *Development*. 2013;140:4237–4245.
30. Shi Q, Gu S, Yu XS, White TW, Banks EA, Jiang JX. Connexin controls cell-cycle exit and cell differentiation by directly promoting cytosolic localization and degradation of E3 ligase Skp2. *Dev Cell*. 2015;35:483–496.
31. Hu Z, Shi W, Riquelme MA, et al. Connexin 50 functions as an adhesive molecule and promotes lens cell differentiation. *Sci Rep*. 2017;7:5298.
32. Chi J, Li L, Liu M, et al. Pathogenic connexin-31 forms constitutively active hemichannels to promote necrotic cell death. *PLoS One*. 2012;7:e32531.
33. Easton JA, Albuloushi AK, Kamps MAF, et al. A rare missense mutation in GJB3 (Cx31G45E) is associated with a unique cellular phenotype resulting in necrotic cell death. *Exp Dermatol*. 2019;28:1106–1113.
34. Wang E, Wang D, Geng A, Seo R, Gong X. Growth of hollow cell spheroids in microbead templated chambers. *Biomaterials*. 2017;143:57–64.
35. Shakespeare TI, Sellitto C, Li L, et al. Interaction between Connexin50 and mitogen-activated protein kinase signaling in lens homeostasis. *Mol Biol Cell*. 2009;20:2582–2592.
36. Martinez JM, Wang HZ, Lin RZ, Brink PR, White TW. Differential regulation of Connexin50 and Connexin46 by PI3K signaling. *FEBS Lett*. 2015;589:1340–1345.

Investigative Ophthalmology & Visual Science